J. Chem. Thermodynamics **1999**, 31, 479–490
Article No. jcht.1998.0464
Available online at http://www.idealibrary.com on IDEAL

JCT

The speed of sound, and derived thermodynamic properties of liquid trifluoromethane (HFC23) from $T = (258$ to $303)$ K at pressures up to 65 MPa

P. F. Pires and H. J. R. Guedes[a]

Departamento de Química, Centro de Química Fina e Biotecnologia, Faculdade de Ciências e Tecnologia, Universidade Nova de Lisboa, P-2825 Monte de Caparica, Portugal

This work reports experimental data of the speed of sound in liquid trifluoromethane (HFC23, or R23) from $T = (258$ to $303)$ K at pressures up to 65 MPa, measured with a pulse-echo method adapted from Papadakis[1] and Guedes *et al.*[2] The results are fitted to a rational approximant and compared with literature data.[3] Derived thermodynamic properties such as the isentropic compressibility κ_s, the isothermal compressibility κ_T, the cubic expansion coefficient α_p, and the specific heat capacity at constant pressure c_p are calculated by combining the present experimental data with the density values published by other authors.[4–11] The estimated properties are compared, where possible, with literature data.

KEYWORDS: speed of sound; alternative refrigerants; trifluoromethane; HFC23; thermodynamic properties.

1. Introduction

Trifluoromethane (HFC23) has been suggested as a replacement for conventional refrigerants[6, 13–15] such as chlorodifluoromethane (HCFC22) and the azeotropic blend HCFC502, $\{x\mathrm{CHClF_2} + (1-x)\,\mathrm{CClF_2CH_3}\}$, of mass fraction composition $\omega(\mathrm{CHClF_2}) = 0.488$,[7–9] as well as CClF3 (CFC13) and the blend HCFC503, $\{x\mathrm{CClF_3} + (1-x)\,\mathrm{CHF_3}\}$, of mass fraction composition $\omega(\mathrm{CCIF_3}) = 0.599$ for low-temperature applications.[11, 16–18] Besides its non-flammability, HFC23 presents no toxicological risks. As it contains no chlorine atoms, its ozone depletion potential is zero. Because of its higher content of hydrogen atoms, its atmospheric lifetime is shorter, resulting in a global warming potential less than half that of CFC13.[5]

In the present work, we report values of the speed of sound u of HFC23 measured with a newly built apparatus, with which the HFC32 speed of sound has recently been measured.[12]

[a]To whom correspondence should be addressed (E-mail: h.guedes@dq.fct.unl.pt).

0021–9614/99/040479 + 12 $30.00/0

The measurements were obtained in the temperature range 258 K to 303 K and pressures up to 65 MPa.

The present speed of sound data together with published density ρ data[4–11] were used to calculate thermodynamic properties such as the isentropic compressibility κ_s, the isothermal compressibility κ_T, the cubic expansion coefficient α_p, and the specific heat capacity at constant pressure c_p.

The calculation method used was quite simple. First, we fitted the experimental speed of sound and density data to selected equations. The aim was to use simple functional forms of the pressure and temperature. The functions should fit accurately the experimental data and, if possible, allow a limited extrapolation of the experimental range, especially in the temperature. Since some thermodynamic properties are calculated from the derivatives of the density, care must be taken to ensure a proper behaviour of the partial derivatives of the chosen function.

To fit the speed of sound and density data, we chose a PADE approximant of the form:

$$F(p, T) = \left(\sum_{i=0}^{N_p} \sum_{j=0}^{N_T} A_{ij} p^i T^j \right) \Bigg/ \left(\sum_{k=0}^{D_p} \sum_{l=0}^{D_T} B_{kl} p^k T^l \right). \tag{1}$$

The isentropic compressibility $\kappa_s = (1/\rho)(\partial\rho/\partial p)_S$ is calculated from the relation:

$$\kappa_S = 1/\rho u^2. \tag{2}$$

The isothermal compressibility and the cubic expansion coefficient defined by equations (3) and (4) were directly calculated from the density and its partial derivatives:

$$\kappa_T = (1/\rho)(\partial\rho/\partial p)_T, \tag{3}$$

$$\alpha_p = -(1/\rho)(\partial\rho/\partial T)_p. \tag{4}$$

The speed of sound can be related to c_p and ρ by the following expression:

$$1/u^2 = (\partial\rho/\partial p)_T - (T/\rho^2 c_p)(\partial\rho/\partial T)_p^2. \tag{5}$$

The rearrangement of equation (5) and its combination with equations (2) to (4) lead to equation (6), which relates the specific heat capacity at constant pressure to the temperature, density, isothermal compressibility, cubic expansion coefficient, and the ratio $\gamma = \kappa_T/\kappa_s$:

$$c_p = (T/\rho) - (\alpha_p^2/\kappa_T)(\gamma/\gamma - 1). \tag{6}$$

As can be seen from both the definition of the isentropic compressibility and from equation (2), the speed of sound can be obtained from the partial derivative of the density with respect to pressure at constant entropy. Therefore, the combination of speed of sound and density data should increase by an order of magnitude the accuracy of the derived thermodynamic properties.

2. Experimental

The speed of sound of liquid HFC23 was measured in an acoustic cell designed for high pressures, using the method described in reference 12. The apparatus use a pulse-echo

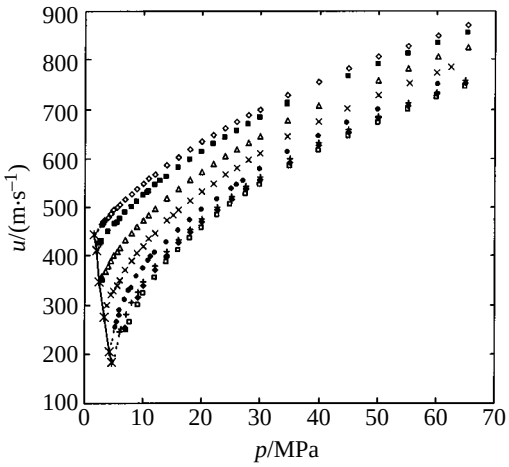

FIGURE 1. Experimental speed of sound u for HFC23 as a function of pressure p at: ◊, $T = 258.19$ K; ■, $T = 263.22$ K; △, $T = 273.10$ K; ×, $T = 283.22$ K; ●, $T = 293.29$ K; +, $T = 298.18$ K; ♦, $T = 299.83$ K; □, $T = 303.25$ K; —×—, saturation line.

method at a frequency of 1 MHz. The accuracy of the speed of sound measurements is estimated to be better than ± 0.4 m·s^{-1} for pressures up to 35 MPa, and ± 1.4 m·s^{-1} for pressures above this value.

The cell was thermostatted inside a Dewar vessel with the help of two cascaded thermostatted baths. The long-term temperature stability of the complete system was within ± 0.02 K, and the temperature measurements were taken with a four-wire platinum resistance thermometer and a digital multimeter. The thermometer was previously calibrated on ITS90 scale and the uncertainty of the temperature measurements was ± 0.01 K.

The pressure was measured with two instruments. In the lower range, from the vapour pressure up to 35 MPa, a Setra Systems Inc. pressure transducer was used. In the higher range (up to $p = 65$ MPa) a Digibar transducer was used. The pressure sensors were calibrated, and the resulting uncertainies were 0.025 MPa for the lower range, and ± 0.2 MPa for the higher range.

The HFC23 used in the experimental work was supplied by Solvay Fluor und Derivate GmbH, with a stated mass fraction purity of 0.9998. The sample was further dried with molecular sieves and degassed three times by freezing with liquid nitrogen, followed by an evacuation of the remaining gas phase (flush out).

3. Results and discussion

The 226 values of the speed of sound of liquid HFC23, along eight isotherms from $T =$ (258 to 303) K and pressures up to 65 MPa, are presented in table 1 and plotted against pressure at different temperatures in figure 1. Although not obvious from figure 1, the temperature dependence of the speed of sound shows an inflection point at high pressures,

TABLE 1. Experimental data of the speed of sound u of HFC23 at temperatures from $T = 258$ K to $T = 303$ K and pressures p up to 65 MPa

T/K	p/MPa	u/m·s^{-1}	T/K	p/MPa	u/m·s^{-1}	T/K	p/MPa	u/m·s^{-1}
258.18	2.88	464.5	258.19	7.90	527.7	258.18	23.99	662.0
258.21	2.99	466.1	258.19	8.90	538.4	258.17	26.00	675.2
258.18	3.11	468.0	258.19	9.90	548.6	258.17	28.00	687.7
258.20	3.20	469.2	258.19	9.90	548.6	258.19	28.00	687.7
258.22	3.29	470.6	258.18	10.91	558.6	258.20	29.98	700.0
258.19	3.40	472.1	258.20	11.91	568.1	258.20	34.65	728.4
258.19	3.95	479.7	258.18	13.93	586.2	258.19	39.81	756.1
258.19	4.43	486.3	258.17	15.94	603.0	258.21	44.97	781.7
258.20	4.98	493.5	258.19	15.94	603.1	258.18	50.03	805.8
258.20	5.45	499.5	258.17	17.96	619.0	258.20	55.19	827.9
258.18	5.90	504.8	258.17	19.97	634.0	258.20	60.35	849.1
258.19	6.90	516.6	258.19	21.98	648.4	258.20	65.42	869.3
263.31	2.54	424.3	263.21	9.90	522.8	263.20	28.00	668.6
263.16	2.57	424.5	263.23	9.90	522.9	263.22	29.98	681.7
263.34	2.73	427.2	263.19	10.59	530.1	263.18	34.65	711.7
263.15	2.78	428.3	263.24	10.91	533.3	263.21	34.65	708.5
263.22	2.88	430.1	263.17	11.91	544.4	263.23	34.65	708.3
263.22	4.09	449.4	263.36	12.92	552.9	263.23	34.65	708.8
263.17	5.12	464.4	263.29	13.93	562.5	263.21	44.97	765.4
263.28	5.45	469.1	263.22	15.94	580.8	263.18	50.03	789.3
263.27	5.90	475.5	263.20	17.96	597.2	263.18	55.19	812.0
263.34	6.90	487.9	263.22	19.97	613.1	263.20	60.35	833.6
263.16	6.93	488.8	263.22	21.98	628.0	263.22	65.42	854.3
263.26	7.90	500.4	263.20	23.99	642.1			
263.33	8.90	511.8	263.20	26.00	655.7			
273.13	2.77	353.7	273.14	7.90	446.5	273.05	26.00	618.4
273.17	2.88	355.6	273.07	8.90	459.8	273.10	28.00	632.1
273.06	2.95	357.9	273.05	9.90	472.5	273.11	29.98	645.2
273.15	3.45	369.6	273.01	10.91	484.9	273.07	34.65	677.6
273.06	3.95	380.4	273.14	11.91	496.4	273.08	39.81	706.8
273.07	4.43	390.0	273.04	13.93	517.6	273.05	50.03	758.9
273.07	4.43	390.0	273.09	15.94	537.2	273.17	50.03	758.9
273.17	4.95	399.4	273.10	17.96	555.5	273.16	55.19	782.4
273.16	5.45	408.7	273.02	19.97	572.6	273.15	60.35	804.9

TABLE 1—*continued*

T/K	p/MPa	u/m·s^{-1}	T/K	p/MPa	u/m·s^{-1}	T/K	p/MPa	u/m·s^{-1}
272.98	5.90	416.0	273.15	21.98	588.8	273.14	65.42	825.4
273.03	6.90	431.8	273.12	23.99	604.0			
283.25	3.48	284.0	283.20	9.90	420.4	283.22	26.00	581.4
283.19	3.84	299.7	283.26	10.91	434.7	283.22	28.00	596.2
283.24	4.54	319.5	283.21	11.91	447.6	283.17	29.98	610.0
283.25	4.95	327.5	283.20	13.93	471.9	283.23	34.65	644.0
283.24	5.45	339.7	283.15	15.15	485.2	283.16	39.81	674.5
283.20	5.90	350.1	283.24	15.94	493.5	283.18	44.77	701.9
283.21	6.90	371.0	283.26	17.96	513.8	283.24	50.03	728.4
283.21	6.90	371.0	283.26	19.97	533.4	283.22	55.29	753.4
283.23	7.90	388.7	283.24	21.98	549.6	283.25	59.95	774.3
283.26	8.90	405.2	283.18	23.99	566.0	283.22	62.38	785.4
293.31	5.31	254.2	293.32	10.91	388.9	293.29	27.00	554.4
293.23	5.45	264.0	293.32	11.39	397.5	293.28	29.99	576.9
293.31	5.90	275.9	293.30	11.92	404.9	293.28	34.65	612.3
293.26	6.06	288.8	293.33	13.93	427.4	293.29	34.65	612.5
293.30	6.90	308.2	293.24	15.94	451.6	293.31	39.81	643.7
293.26	6.91	308.1	293.26	17.96	473.7	293.28	44.77	672.7
293.31	7.64	327.1	293.29	19.97	493.8	293.27	50.03	699.8
293.26	7.90	332.7	293.29	22.50	517.2	293.28	60.35	749.0
293.28	8.90	357.3	293.27	25.00	538.1			
293.32	9.90	372.6	293.26	26.00	546.4			
298.14	6.06	244.9	298.14	16.00	432.6	298.17	39.91	630.4
298.17	6.28	249.9	298.21	18.00	455.3	298.22	44.97	659.0
298.17	7.00	279.1	298.13	20.00	476.1	298.22	50.03	685.8
298.12	8.00	304.9	298.10	22.50	500.0	298.25	55.09	711.8
298.13	9.00	324.8	298.11	25.00	522.2	298.26	59.95	734.5
298.16	10.00	348.3	298.24	27.50	542.0	298.26	65.01	757.0
298.17	12.00	378.5	298.23	30.00	560.9			
298.16	14.00	407.4	298.23	35.05	599.2			
299.85	6.80	252.0	299.86	16.00	428.8	299.82	35.05	591.4
299.82	8.98	314.8	299.83	18.00	448.7	299.82	39.91	625.5
299.87	10.00	339.1	299.82	20.00	469.8	299.84	44.97	654.3
299.82	12.00	370.7	299.79	22.50	494.0	299.83	50.03	681.5

TABLE 1—*continued*

T/K	p/MPa	u/m·s^{-1}	T/K	p/MPa	u/m·s^{-1}	T/K	p/MPa	u/m·s^{-1}
299.82	13.93	399.4	299.83	25.00	515.8	299.82	55.09	707.2
299.81	13.93	398.9	299.81	27.50	536.6	299.84	59.95	729.9
299.87	14.00	400.0	299.83	30.00	555.8	299.85	65.01	752.4
303.24	7.16	246.9	303.24	18.01	436.2	303.25	39.91	615.7
303.23	7.65	264.0	303.24	20.00	457.7	303.27	44.97	644.9
303.25	8.98	297.8	303.25	22.50	482.6	303.29	50.03	672.6
303.25	10.00	321.5	303.24	24.73	504.9	303.24	55.09	698.1
303.26	11.99	354.9	303.23	27.50	525.6	303.24	59.95	721.9
303.25	14.00	386.0	303.23	30.00	545.2	303.24	65.01	744.3
303.24	16.00	412.7	303.24	35.05	584.4			

TABLE 2. Parameters of equation (1) used to fit the speed of sound data with $N_p = N_T = D_p = D_T = 3$

A_{ij}	j		
i	0	1	2
0	$2.5988813\cdot10^{3}$	$380312\cdot10^{1}$	$439497\cdot10^{-2}$
1	$-1.4810105\cdot10^{2}$	$552315\cdot10^{0}$	$467355\cdot10^{-3}$
2	$3.4623611\cdot10^{-1}$	$656440\cdot10^{-3}$	$540514\cdot10^{-5}$

B_{kl}	l		
k	0	1	2
0	$1.0000000\cdot10^{0}$	$839322\cdot10^{-3}$	$390505\cdot10^{-6}$
1	$-7.4504732\cdot10^{-2}$	$503708\cdot10^{-4}$	$402817\cdot10^{-7}$
2	$9.9202472\cdot10^{-4}$	$936492\cdot10^{-5}$	$891337\cdot10^{-8}$

similar to the one observed for the density values of Rubio *et al.*[4] A few measurements were randomly repeated, yielding a precision of ±0.1 m·s^{-1}. We have fitted the data to equation (1) and obtained an overall standard deviation of 1.2 m·s^{-1}, which corresponds to an uncertainty of ±0.18 per cent.

In figure 2 we have plotted the per cent deviations of the experimental data from the fit. It can be seen from this figure that larger deviations occur at speed of sound values below 400 m·s^{-1}. These correspond to measurements made in the near critical region $\{T_c = (299.01 \pm 0.01)$ K, $p_c = (4.8162 \pm 0.0018)$ MPa$\}$.[5] It is believed that this problem is caused by several factors. One of them is the larger attenuation of the acoustic pulse, which decreases the signal to noise ratio at the output of the piezoelectric transducer, thus making measurements rather more difficult. Furthermore, because of the proximity to the critical point, density gradients along the acoustic path are expected to rise. As a matter

TABLE 3. Speed of sound u_σ of liquid HFC23 extrapolated to saturation pressures p_σ at the saturation temperature T

T / K	p_σ / MPa	u_σ / m·s^{-1}
258.19	1.639	444.0
263.23	1.902	411.4
273.23	2.506	346.1
283.22	3.272	274.2
293.29	4.218	204.6
298.18	4.762	182.7

TABLE 4. Parameters of equation (1) used to fit the liquid HFC23 density data with $N_p = N_T = D_p = D_T = 3$

A_{ij}	j		
i	0	1	2
0	$1.8301442\cdot10^{3}$	$-1.1038737\cdot10^{1}$	$1.6277468\cdot10^{-2}$
1	$-1.2374701\cdot10^{1}$	$1.9045560\cdot10^{-1}$	$-4.3436162\cdot10^{-4}$
2	$1.2151955\cdot10^{-2}$	$6.8622002\cdot10^{-4}$	$3.7851435\cdot10^{-6}$

B_{kl}	l		
k	0	1	2
0	$1.0000000\cdot10^{0}$	$-5.3490934\cdot10^{-3}$	$6.5896372\cdot10^{-6}$
1	$-7.3929047\cdot10^{-3}$	$1.0452925\cdot10^{-4}$	$-1.9956084\cdot10^{-7}$
2	$3.1648650\cdot10^{-5}$	$6.8564084\cdot10^{-7}$	$2.9375044\cdot10^{-9}$

of fact, near the critical point, as the relaxation processes become slower, we expect the experimental ultrasonic speeds of sound not to be as accurate as elsewhere in the region, where the deviation from the thermodynamic zero frequency speed of sound is well below the experimental error. As can be seen in figure 2, deviations as great as 1.5 per cent occur near the critical point and, consequently, the results are less reliable.

We have compared our results with those of Takagi,[3] who reported about 80 speed of sound measurements between $T =$ (235.15 and 333.15) K and pressures up to 35 MPa, along seven isotherms. Within the (p, T) region where both data sets overlap — three isotherms at $T =$ (263.15, 283.15, and 298.15) K — average deviations from the author's data of 0.43 per cent, 0.60 per cent, and 1.26 per cent, respectively, were obtained on each isotherm, with the deviations decreasing at higher pressures. Again, as expected, larger deviations occur at lower pressures and higher temperatures, *i.e.* near the critical region.

Table 3 shows values of the liquid speed of sound at saturation conditions. Since part of the apparatus is at room temperature, our lower pressure limit was the vapour pressure at

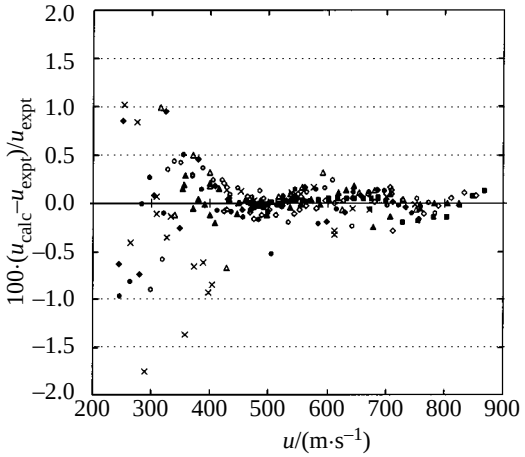

FIGURE 2. Deviations per cent $\{100\cdot(u_{calc} - u_{expt})/u_{expt}\}$ of the calculated speed of sound values using equation (1) with the parameters of table 2 from corresponding experimental data as a function of the speed of sound u at: ■, $T = 258.19$ K; ◊, $T = 263.22$ K; ▲, $T = 273.10$ K; ○, $T = 283.22$ K; ×, $T = 293.29$ K; ♦, $T = 298.18$ K; △, $T = 299.83$ K; ●, $T = 303.25$ K.

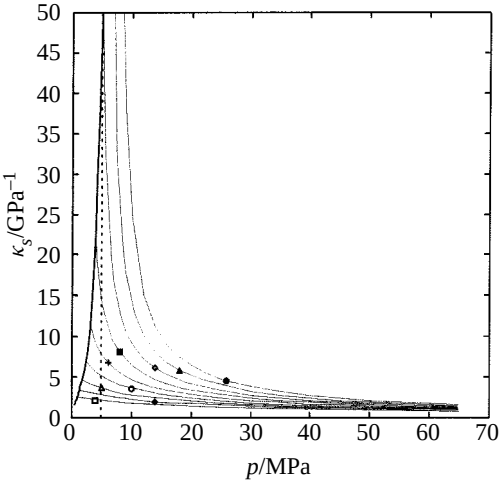

FIGURE 3. Calculated isoentropic compressibility κ_S of HFC23 as a function of pressure p at: □, $T = 240$ K; ♦, $T = 250$ K; △, $T = 260$ K; ●, $T = 270$ K; +, $T = 280$ K; ■, $T = 290$ K; ◊, $T = 300$ K; ▲, $T = 310$ K; ○, $T = 320$ K; ·····, critical pressure; ——, saturation line.

this temperature. Thus, we were unable to reach saturation pressures at temperatures below $T = 298$ K. Therefore, all u_σ values were determined by extrapolation of each isotherm to the saturation pressure. The uncertainty in the u_σ data is estimated to be better than ± 1.0 m·s^{-1}, except near the critical point.

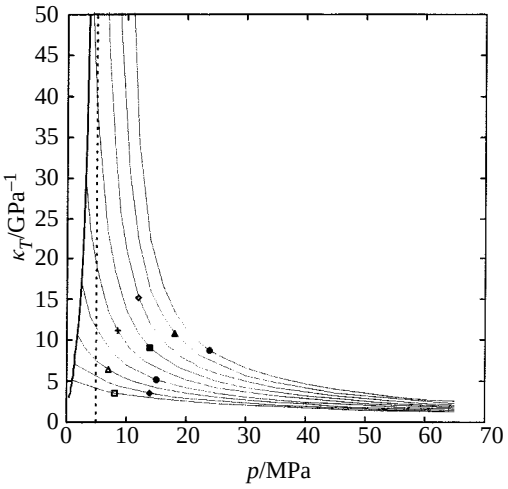

FIGURE 4. Calculated isothermal compressibility κ_T of HFC23 as a function of pressure p at: □, $T = 240$ K; ♦, $T = 250$ K; △, $T = 260$ K; •, $T = 270$ K; +, $T = 280$ K; ■, $T = 290$ K; ◊, $T = 300$ K; ▲, $T = 310$ K; ○, $T = 320$ K; ·····, critical pressure; ——, saturation line.

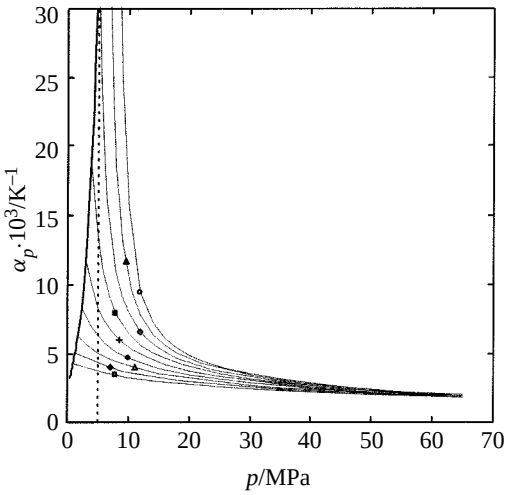

FIGURE 5. Calculated cubic expansion coefficient α_p of HFC23 as a function of pressure p at: □, $T = 240$ K; ♦, $T = 250$ K; △, $T = 260$ K; •, $T = 270$ K; +, $T = 280$ K; ■, $T = 290$ K; ◊, $T = 300$ K; ▲, $T = 310$ K; ○, $T = 320$ K; ·····, critical pressure; ——, saturation line.

For the density data, we have used the same rational approximant {equation (1)} as for the speed of sound data. The parameters of the fit are presented in table 4. The region covered extended from $T = (125$ to $350)$ K, and from the vapour pressure up to 90 MPa, with a total of 292 experimental values obtained from literature.[4–11] The standard deviation of this fit is 3.5 kg·m^{-3}.

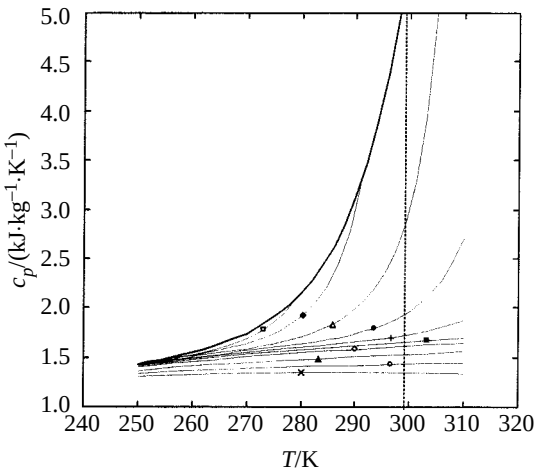

FIGURE 6. Calculated specific heat capacity at constant pressure c_p of liquid HFC23 as a function of temperature T at: □, $p = 3$ MPa; ♦, $p = 4$ MPa; △, $p = 5$ MPa; •, $p = 6$ MPa; +, $p = 8$ MPa; ■, $p = 10$ MPa; ◊, $p = 20$ MPa; ▲, $p = 30$ MPa; ○, $p = 40$ MPa; ×, $p = 50$ MPa; ·····, critical temperature; ——, saturation line.

TABLE 5. Calculated values of the specific heat capacity c_p for HFC23 at rounded values of pressure p and temperature T

p/MPa	T/K						
	250	260	270	280	290	300	310
1.5	1.43						
2	1.43	1.54	1.77				
3	1.43	1.53	1.69	2.15			
5	1.43	1.51	1.61	1.78	2.30		
8	1.43	1.50	1.56	1.63	1.74	1.96	2.71
10	1.42	1.49	1.55	1.60	1.66	1.73	1.87
15	1.39	1.45	1.50	1.55	1.58	1.61	1.64
20	1.36	1.41	1.45	1.48	1.50	1.53	1.56
25	1.33	1.37	1.39	1.41	1.42	1.43	1.45
30	1.31	1.33	1.34	1.35	1.35	1.34	1.34

Combining both fits (speed of sound and density), we have calculated the isentropic compressibility by using equation (2). We estimate the accuracy of the isentropic compressiblity to be ± 0.3 per cent at pressures up to 35 MPa, and ± 0.75 per cent above this pressure. The results are shown in figure 3. Takagi[3] presented the results of the isentropic compressibility in graphical form and thus they could not be quantitatively compared with our results. From

a comparison with values read from the graph, their agreement with ours is found to be within ±2 per cent.

Both the isothermal compressibility (figure 4) and the cubic expansion coefficient (figure 5) were calculated by analytical derivation of equation (1) and by using equations (3) and (4). In view of the high quality of the available density data and the analytical method used for the derivatives, we estimate an accuracy of ±0.4 per cent for the isothermal compressiblity and the cubic expansion coefficient. Our results were compared with those of Rubio *et al.*[4] and we found deviations from them of the order of ±1.0 per cent, reaching ±3.0 per cent near the critical region. Usually, the type of equation used by Rubio *et al.*[4] deviates strongly from the experimental results near the critical region.

The specific heat capacity at constant pressure was calculated by using equation (6), with an estimated uncertainty of ±1.0 per cent. Table 5 shows c_p data at rounded values of pressure and temperature. Figure 6 presents the results of 11 isobars ranging from the saturation line up to $p = 60$ MPa. There is a locus of extrema in the pressure dependence of c_p, reflecting a line of inflection points in the temperature dependence of the density values of Rubio *et al.*[4] This behaviour is accounted for by the thermodynamic relation:

$$(\partial c_p/\partial p)_T = -T(\partial^2 V_m/\partial T^2)_p, \tag{7}$$

where V_m is the molar volume.

As far as we know, there are no literature values of c_p for liquid HFC23 with which to compare our calculated values. The calculation method, involving the combination of speed of sound and density data, allows the calculation of other thermodynamic properties to be made with more accuracy than simply on the basis of density data. This is especially important in the case of properties such as c_p, which is difficult to measure under difficult experimental conditions such as high pressures. The speed of sound and density data can also be combined with accurate c_p values at lower pressures to develop appropriate equations of state for pure fluids and mixtures.

P.F. Pires wishes to thank the Fundação para a Ciência e Tecnologia (grant BD/2522/93/RM). We are also grateful to Solvay Fluor and Derivate GmbH for providing us with the refrigerant sample.

REFERENCES

1. Papadakis, E. P. *J. Acoust. Soc. Am.* **1967**, 42, 1045–1051.
2. Guedes, H. J. R.; Zollweg, J. A. *Int. J. Refrig.* **1992**, 15, 381–385.
3. Takagi, T. 14th Japan Symposium on Thermophysical Properties, Yokohama, Japan (in Japanese). **1993**, pp. 287–290.
4. Rubio, R. G.; Zollweg, J. A.; Palanco, J. M. G.; Calado, J. C. G; Miller, J.; Streett, W. B. *J. Chem. Eng. Data* **1991**, 36, 171–184.
5. Rubio, R. G.; Zollweg, J. A.; Streett, W. B. *Ber. Bunsenges. Phys. Chem.* **1989**, 93, 791–800.
6. Aizpiri, A. G.; Rey, A.; Dávila, J.; Rubio, R. G.; Zollweg, J. A.; Streett, W. B. *J. Phys. Chem.* **1991**, 95, 3351–3357.
7. Ohgaki, K.; Umezono, S.; Katayama, T. *J. Supercritical Fluids* **1990**, 3, 78–84; Valentine, R. H.; Brodale, G. E.; Giauque, W. F. *J. Phys. Chem.* **1962**, 66, 392–395.
8. Hori, K.; Okazaki, S.; Uematsu, M.; Watanabe, K. Proc. 8th Symposium on Thermophysical Properties. Sengers, J. V.: editor. Gaithesburg, MD, U.S.A. **1982**, pp. 380–386.

9. Wagner, W. *Kaeltetechnik-Klimatisierung* **1968**, 20, 238–240; Iglesias-Silva, G. A.; Miller, R. C.; Ceballos, A. D.; Hall, K. R.; Holste, J. C. *Fluid Phase Equilib.* **1995**, 111, 203–212.
10. Belzile, J. L.; Kaliaguine, S.; Ramalho R. S. *Can. J. Chem. Eng.* **1976**, 54, 446–450.
11. SOLVAY FLUOR UND DERIVATE leaflet on Refrigerant 23. **1997**.
12. Pires, P. F.; Guedes, H. J. R. *J. Chem. Thermodynamics* **1999**, 31, 55–69.
13. Sato, H.; Watanabe, K. 19th International Congress of Refrigeration, International Institute of Refrigeration (IIR/IIF). The Hague, The Netherlands. **1995**, IVa, pp. 519–526.
14. Cohen, R.; Groll, E. *Bull. Int. Inst. Refrigeration (IIR/IIF)* **1996**, 96.5, 3–19.
15. Weiss, P.; Barreau, M.; Macaudiere, S. 19th International Congress of Refrigeration, International Institute of Refrigeration (IIR/IIF), The Hague, The Netherlands. **1995**, IVa, pp. 606–613.
16. Lisál, M.; Vacek, V. *Fluid Phase Equilib.* **1996**, 118, 61–76.
17. Hall, R. L.; Battelle; Johnson, M. R. Proceedings of the 1994 International Refrigeration Conference at Purdue. Purdue University, W. Lafayette, IN, U.S.A. **1994**, pp. 183–189.
18. Paulus-Lanckriet, M.; Balthasart, D. 19th International Congress of Refrigeration, International Institute of Refrigeration (IIR/IIF), The Hague, The Netherlands, **1995**, IVa, pp. 472–480.

(Received 18 May 1998; in final form 13 November 1998)

WA98/024